JPEDAV (2004) 25:515-519
DOI: 10.1361/15477020421241
1547-7037/$19.00 ©ASM International

# Thermodynamics of Phase Changes in Systems BaS-$Ln_2S_3$ (Ln = Pr, Sm, Gd, Tb, Er, Lu)

***N.A. Khritohin, O.V. Andreev, O.V. Mitroshin, and A.S. Korotkov***

*(Submitted April 15, 2002; in revised form August 31, 2004)*

**Thermodynamic analyses of phase changes were carried out for the systems BaS-$Ln_2S_3$ with Ln = Pr, Sm, Gd, Tb, Er, and Lu, and the phase diagrams have been experimentally constructed. Formation of the $Ba_3Ln_2S_6$ sulfides with Ln = Tb through Lu was predicted from the thermodynamic behavior of melts, and the existence of these phases has been experimentally confirmed. Heats of melting were estimated for the sulfides $Ln_2S_3$, $BaLn_2S_4$, and $Ba_3Ln_2S_6$.**

## 1. Experimental Approach

The phase diagrams of the systems BaS-$Ln_2S_3$ with Ln = Pr, Sm, Gd, Tb, Er, and Lu have been experimentally constructed (Ref 1, 2). The diagrams of BaS-$Pr_2S_3$, BaS-$Sm_2S_3$, BaS-$Tb_2S_3$, and BaS-$Lu_2S_3$ are shown in Fig. 1 as representative examples. Extended terminal solid solutions of BaS in $Ln_2S_3$ were observed for the lighter lanthanons in the lanthanide series La through Lu, wherein both atomic numbers and atomic weights monotonically increase from La to Lu but atomic sizes decrease. In the specific case of Ln = Pr, the terminal solution of BaS in $Ln_2S_3$ extends to approximately equimolar stoichiometry and in the BaS-rich region of the solution, the crystal structure tends to order with a $Th_3P_4$-type structure. The compound $BaLn_2S_4$ is formed in the phase diagrams of Ln = Sm, Gd, Tb, Er, and Lu; the compound $Ba_3Ln_2S_6$ is additionally formed in the phase diagrams of Ln = Tb, Er, and Lu; and a third compound, $BaLu_8S_{13}$, is formed in the BaS-$Lu_2S_3$ system.

Experimental determinations of the heats of melting of these sulfide compounds have not been done because measurements are difficult with large heat values and with melting occurring in the temperature range ~1900 K and above. Estimation of these heats of melting can be estimated thermodynamically from the temperature-composition trends of the equilibrium phase boundaries determined for the construction of the phase diagrams. Thermodynamic analysis of an equilibrium solution boundary, in the present case a melt solution boundary, allows one to predict phase formation from the deviation of the solution from ideality. The validity of such predictions can be tested by experiment. For the present purposes, interest is in the contours of the liquidus in equilibrium with one or another of the solid sulfides. The work was undertaken to estimate heats of melting of the solid sulfides from the thermodynamic relationships between such heats and the compositional differences between liquidus and solid phases across equilibrium two-phase regions.

## 2. Estimated Heats of Melting (Fusion)

The compounds $BaLn_2S_4$ that occur in the heavier lanthanon systems have been found to melt congruently and for experimentally determined systems wherein a eutectic reaction occurs between $BaLn_2S_4$ and $Ln_2S_3$. Estimates of the heats of melting of these two compounds were made from the compositional difference between liquidus and compound at temperatures between the eutectic temperature, $T_{eu}$, and compound melting, $T_m$, and in the composition region between the eutectic, $X_{eu}$, and the solid phase boundary, $X_c$. Other regions between compounds were treated analogously. The experimental thermal analysis data for compositions were used to estimate heats of melting with Van Laar's equation in the form

$$\ln (X_i^L/X_i^S) = (\Delta H_m/R)[(1/T_m) - (1/T)] \qquad \text{(Eq 1)}$$

where $R$ is the gas constant, $\Delta H_m$ is the heat of melting of the $i$th compound of interest, $X_i$ is the mole fraction of the $i$th compound, the superscripts L and S represent liquid and solid, respectively, $T_m$ is defined above, and $T$ is the temperature at which the $X_i^S$ are evaluated. In the temperature range between $T_{eu}$ and $T_m$, $\Delta H_m$ can be taken as a constant so Eq 1 can be rearranged in linear form to define a relationship defining $T^{-1}$ in terms of $\ln (X_i^L/X_i^S)$ to develop a set of relations from experimental conodes for evaluation of $\Delta H_m$ by utilizing a regression method. Results of such estimates for $Ln_2S_3$ are given in Table 1 and for $BaLn_2S_4$ in Table 2.

**Table 1 Estimates of the heats of melting in simple sulfides**

| Sulfide | $\Delta H$, kJ/mol |
|---|---|
| $Lu_2S_3$ | 684 |
| $Er_2S_3$ | 152 |
| $Tb_2S_3$ | 94 |
| $Gd_2S_3$ | 60 |
| $Sm_2S_3$ | 88 |
| $Pr_2S_3$ | 94 |
| BaS | 57 |

---

**N.A. Khritohin, O.V. Andreev, O.V. Mitroshin,** and **A.S. Korotkov,** Tyumen State University, Semakova St. 10, Tyumen 625003, Russia. Contact e-mail: koran@fromru.com.

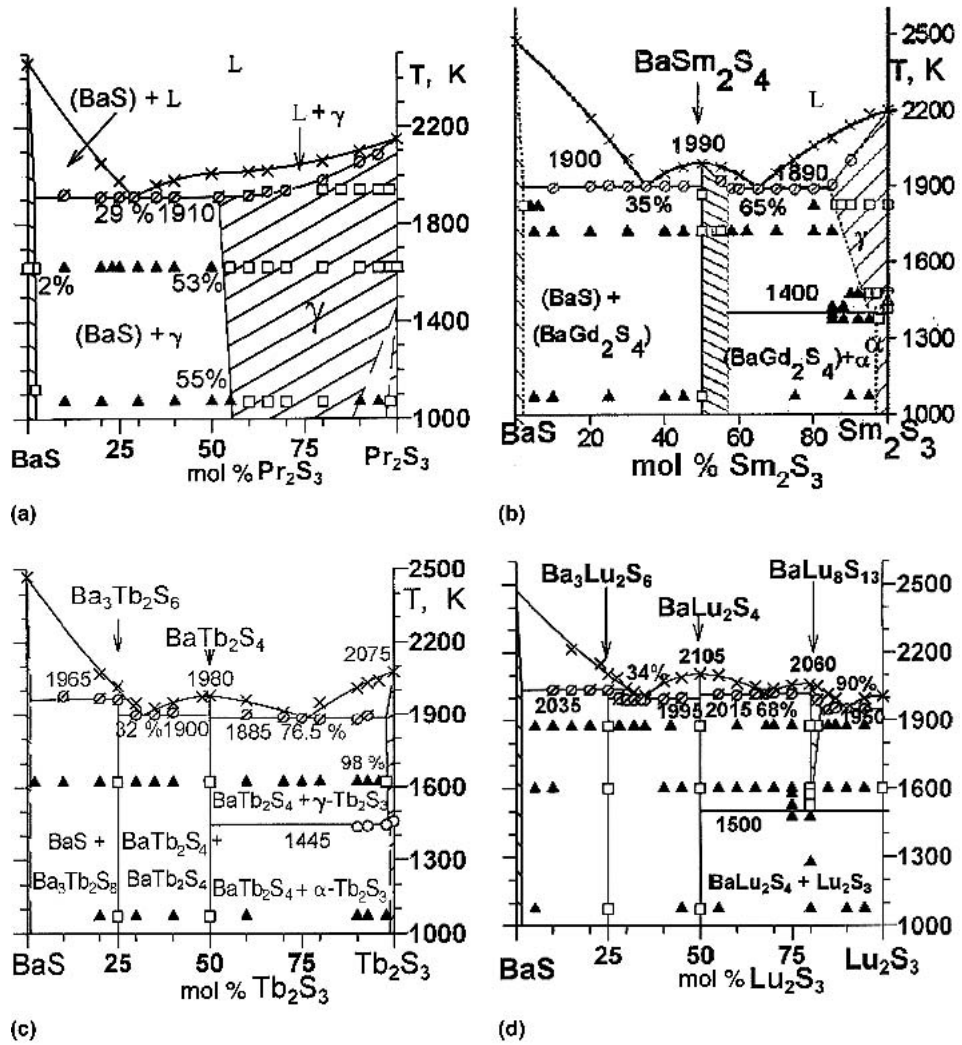

**Fig. 1** Representative phase diagrams of BaS-$Ln_2S_3$ systems for Ln = **(a)** Pr, **(b)** Sm, **(c)** Tb, and **(d)** Lu illustrating the changing patterns of phase equilibria across the lanthanide series. X-ray and microstructural analyses were used to determine the phase fields with symbols (▲) representing two-phase regions and (□) representing single-phase regions. Thermal analyses were used to determine (○) phase transitions, (Ø) onset of melting, and (×) complete melting.

These estimates of $\Delta H_m$s are, as a whole, in agreement with other information (Ref 3, 4). Nevertheless it is necessary to note the obviously high values from the estimates for simple $Ln_2S_3$ sulfides for Ln = Er and Lu at heavy end of the lanthanon series. These high values are believed to be caused by experimental difficulties that limit accurate determination of the compositional liquidus-solidus ratio at the $Ln_2S_3$-rich end of the phase diagrams. Nevertheless there is without doubt a considerable decrease in $\Delta H_m$ for each sulfide in the progression from Lu downward toward La. This correlates with a decrease in hardness of $Ln^{3+}$ when viewed as Pearson's acid particles (Ref 5) and reflects the degree of filling of 4*f* electronic states. It may be noted that the ranges of homogeneity of the intermediate compounds are quite limited and that the decrease in values of $\Delta H_m$ from system to system in Tables 1 and 2 are consistent with the trends in values of $T_m - T_{eu}$ and $X_{eu} - X_{comp}$ with regard to the position of a lanthanon in the series. These differences combine to produce the observed trend of decrease in $\Delta H_m$ through the progression from Lu toward La. If $\Delta H_m$ of $BaTb_2S_4$ is regarded as an anomaly and the $\Delta H_m$ values in Table 2 are plotted against atomic number or against the radius of the lanthanide ion $r_{Ln^{3+}}$, $\Delta H_m$ drops

**Table 2 Estimates of the heats of melting in binary sulfides**

| Sulfide | $\Delta H$ ($BaLn_2S_4$), kJ/mol |
|---|---|
| $BaLu_2S_4$ | 307 |
| $BaEr_2S_4$ | 264 |
| $BaTb_2S_4$ | 358 |
| $BaGd_2S_4$ | 94 |
| $BaSm_2S_4$ | 84 |

below zero before Pr is reached, and it may be observed that, in the BaS-$Pr_2S_3$ phase diagram, $BaPr_2S_4$ does not occur.

## 3. Excess Partial Molar Gibbs Energies

A thermodynamic estimation of the deviation from ideality of the component compounds forming BaS-$Ln_2S_3$ liquids were done by combining experimental data from thermal analyses with the Van Laar equation in the form

$$\bar{G}_i^{E} = (\Delta H_m/T_m)(T - T_m) + RT \ln (X_i^S/X_i^L) \qquad \text{(Eq 2)}$$

where $\bar{G}_i^{E}$ is the excess partial molar Gibbs energy of the component of interest in the melt, with $X_r^S$ and $X_f^L$ defined as before with $i$ being the compound of interest. Except for the Pr system, data for $X_t^S$ for the solidus end of a conode were obtained by fitting the limited number of experimental datum points to second-degree polynomials by the method of least squares. This allows interpolation to evaluate $X_i^S$ values at desired temperature points to define conodes for the available experimental liquidus points. Fitting was done with a complex program, Phase Gramer, which also evaluated all thermodynamic values of interest.

Results from this estimating procedure are shown in Table 3 for the BaS-$Pr_2S_3$ system; note that the scale for the compositions of BaS invert the scales of Fig. 1 with $X_{BaS}$ for pure BaS being 1 rather than 0. From this table it is evident that for BaS the melt is characterized by a negative deviation from ideality. For the eutectic, the data indicate an excess integral Gibbs energy of $G^E = -5.9$ kJ/mol and produce a Hildebrand energy of interchange reaction of $A_G = -28.4$ kJ/mol. The temperature dependence of $\bar{G}^E_{BaS}$ is

**Table 3 Excess partial Gibbs energies of BaS and $Pr_2S_3$ in the BaS-$Pr_2S_3$ systems**

| Temperature and compositions of liquidus and solidus in region between BaS and eutectic | | | | Temperature and compositions of liquidus and solidus in region between $Pr_2S_3$ and eutectic | | | |
|---|---|---|---|---|---|---|---|
| $T$, K | $X^L_{BaS}$ | $X^S_{BaS}$ | $\bar{G}^E_{BaS}$, kJ/mol | $T$, K | $X^L_{Pr_2S_3}$ | $X^S_{Pr_2S_3}$ | $\bar{G}^E_{Pr_2S_3}$, kJ/mol |
| | | | | 2100 | 0.90 | 0.95 | −1.2 |
| | | | | 2070 | 0.80 | 0.91 | −1.3 |
| 2060 | 0.80 | 0.98 | −6.0 | 2060 | 0.80 | 0.89 | −2.1 |
| 2050 | 0.80 | 0.98 | −6.2 | | | | |
| | | | | 2020 | 0.65 | 0.85 | −1.2 |
| | | | | 2015 | 0.60 | 0.85 | −0.1 |
| | | | | 2010 | 0.60 | 0.85 | −0.3 |
| | | | | 2010 | 0.50 | 0.83 | 2.3 |
| 1980 | 0.75 | 0.98 | −6.9 | 1980 | 0.40 | 0.80 | 4.0 |
| | | | | 1960 | 0.35 | 0.73 | 3.7 |
| | | | | 1955 | 0.35 | 0.73 | 3.4 |
| | | | | 1910 | 0.29 | 0.55 | −0.3 |
| | | | | | 0.29 | 0.54 | −0.6 |
| | | | | | 0.29 | 0.52 | −1.2 |
| | | | | | 0.29 | 0.52 | −1.2 |
| | | | | | 0.29 | 0.52 | −1.2 |
| 1910 | 0.71 | 0.98 | −7.8 | | 0.29 | 0.50 | −1.8 |

**Table 4 Excess partial Gibbs energies of the phase components of melts in the systems of BaS-$BaLn_2S_4$**

| Temperature and compositions of liquidus and solidus in region between BaS and eutectic | | | | Temperature and compositions of liquidus and solidus in region between $BaLn_2S_4$ and eutectic | | | |
|---|---|---|---|---|---|---|---|
| $T$, K | $X^L_{BaS}$ | $X^S_{BaS}$ | $\bar{G}^E_{BaS}$, kJ/mol | $T$, K | $X^L_{BaLn_2S_4}$ | $X^S_{BaLn_2S_4}$ | $\bar{G}^E_{BaLn_2S_4}$, kJ/mol |
| **BaS-$BaSm_2S_4$** | | | | **BaS-$BaSm_2S_4$** | | | |
| 2170 | 0.60 | 0.98 | 1.9 | 1975 | 0.90 | 1.00 | 1.1 |
| 2085 | 0.50 | 0.98 | 2.8 | 1950 | 0.80 | 1.00 | 1.9 |
| 2010 | 0.40 | 0.96 | 4.0 | 1900 (eut.) | 0.70 | 1.00 | 1.8 |
| 1900 (eut.) | 0.30 | 0.96 | 5.2 | | | | |
| **BaS-$BaGd_2S_4$** | | | | **BaS-$BaGd_2S_4$** | | | |
| 2200 | 0.70 | 0.98 | −0.1 | 1990 | 0.90 | 1.00 | 1.3 |
| 2100 | 0.60 | 0.98 | 0 | 1960 | 0.80 | 1.00 | 1.8 |
| 2005 | 0.50 | 0.96 | 0.1 | 1915 | 0.70 | 1.00 | 1.7 |
| 1950 | 0.40 | 0.96 | 2.2 | 1890 (eut.) | 0.66 | 1.00 | 1.7 |
| 1890 (eut.) | 0.34 | 0.96 | 2.9 | | | | |

well described by a linear relationship, $\bar{G}^{\mathrm{E}}_{\mathrm{BaS}} = \bar{H}^{\mathrm{E}}_{\mathrm{BaS}} - T\bar{S}^{\mathrm{E}}_{\mathrm{BaS}}$, with parameters $\bar{H}^{\mathrm{E}}_{\mathrm{BaS}} = 30$ kJ/mol and $\bar{S}^{\mathrm{E}}_{\mathrm{BaS}} = -12$ J/mol · K with a correlation coefficient of $r > 0.99$. From the BaS-$Pr_2S_3$ diagram in Fig. 1 it is evident that the $Pr_2S_3$-rich liquidus has two inflections, which reflects in Table 3 as negative deviations from ideality above 50 mol% $Pr_2S_3$ and below ~30 mol% $Pr_2S_3$ but with positive deviations in the region between. Such positive deviations indicate that intermediate phases should not form in the 35-50 mol% $Pr_2S_3$ region of this system and accounts for the absence of $BaPr_2S_4$ in this system. The reversion to negative deviations at compositions below 30 mol% make likely the existence of associates in the liquid phase with the rapid decrease in the negative interaction pointing to a ratio of 3:1 for the BaS:$Pr_2S_3$ ratio and is indicative of the possible existence of phases such as $Ba_3Ln_2S_6$ in the systems with heavier lanthanons.

The estimating procedure was also applied to other BaS-$Ln_2S_3$ systems. Results for the Sm and Gd systems are shown in Table 4. Excess integral Gibbs energies and Hildebrand energies of exchange are: for the BaS-$Sm_2S_3$ system $G^{\mathrm{E}} = 2.9$ kJ/mol and $A_{\mathrm{G}} = 13.6$ kJ/mol and for BaS-$Gd_2S_3$ system $G^{\mathrm{E}} = 1.9$ kJ/mol and $A_{\mathrm{G}} = 8.4$ kJ/mol. In both systems the melts are characterized by positive deviations from ideality. The temperature dependence of $\bar{G}^{\mathrm{E}}_{\mathrm{BaS}}$ is for both systems well described by linear relationships of the form $\bar{G}^{\mathrm{E}}_{\mathrm{BaS}} = \bar{H}^{\mathrm{E}}_{\mathrm{BaS}} - T\bar{S}^{\mathrm{E}}_{\mathrm{BaS}}$ with parameters $\bar{H}^{\mathrm{E}}_{\mathrm{BaS}} = 29$ kJ/mol and $\bar{S}^{\mathrm{E}}_{\mathrm{BaS}} = -13$ J/mol · K with a correlation coefficient of >0.99 for the BaS-$Sm_2S_3$ system and $\bar{H}^{\mathrm{E}}_{\mathrm{BaS}} = 21$ kJ/mol and $\bar{S}^{\mathrm{E}}_{\mathrm{BaS}} = 9.8$ J/mol · K with a correlation coefficient of 0.86 for the BaS-$Gd_2S_3$ system. The decreasing positive deviation from ideality in progressing from Sm to Gd leads to expectation of additional compounds in heavier lanthanons. An estimate of likely stoichiometry can be made by noting that, up to about 75 mol% BaS in the BaS-$Gd_2S_3$ system, the melt is nearly ideal, but at lower BaS compositions Table 4 shows that there is a sharp increase by an order of magnitude in $\bar{G}^{\mathrm{E}}_{\mathrm{BaS}}$. This means that the preferable composition for the formation of an intermediate phase in the next heavier lanthanon is $Ba_3Ln_2S_6$ at a BaS:$Ln_2S_3$ ratio of 3:1. This prognosis is in agreement with the indications in the results from the BaS-$Sm_2S_3$ system, and such a phase has been found in the BaS-$Tb_2S_3$ system and in all heavier lanthanon systems.

Table 5 shows excess integral Gibbs energies and Hildebrand energies for the series Ln = Gd, Tb, Er in BaS-$Ln_2S_3$ alloys. There is a decrease in both the integral molar Gibbs energy and in the Hildebrand energy from one element to the next. This allows the prediction that an additional phase should exist for heavier lathanons with anticipation that it might occur in the next lanthanon in the series, which is Tm. It has already been shown that such a compound occurs for Lu at a stoichiometry of $BaLu_8S_{13}$. Again in the BaS-$Er_2S_3$ system the partial molar Gibbs energy $\bar{\mathrm{G}}^{\mathrm{E}}_{\mathrm{BaEr_2S_4}}$ is well fit by a linear relationship with $\bar{\mathrm{H}}^{\mathrm{E}}_{\mathrm{BaEr_2S_4}} = -120$ kJ/mol and $\bar{\mathrm{S}}^{\mathrm{E}}_{\mathrm{BaLn_2S_4}} = -57$ J/mol · K with a correlation coefficient of 0.99.

**Table 5 Excess integral Gibbs energies and interchange energies at eutectic temperatures and compositions in $BaLn_2S_4$-$Ln_2S_3$ systems**

| System | $G^{\mathrm{E}}$, kJ/mol | $A_{\mathrm{G}}$, kJ/mol |
|---|---|---|
| $BaGd_2S_4$-$Gd_2S_3$ | 1.5 | 6.2 |
| $BaTb_2S_4$-$Tb_2S_3$ | −2.2 | −8.8 |
| $BaEr_2S_4$-$Er_2S_3$ | −4.4 | −17.8 |

**Table 6 Excess partial molar Gibbs energies of components in the $BaLu_2S_4$-$BaLu_8S_{13}$ system**

| Compositions between eutectic and $BaLu_2S_4$ | | | | Compositions between $BaLu_8S_{13}$ and eutectic | | | |
|---|---|---|---|---|---|---|---|
| $T$, K | $X^{\mathrm{L}}_{\mathrm{BaLu_2S_4}}$ | $X^{\mathrm{S}}_{\mathrm{BaLu_2S_4}}$ | $\bar{G}^{\mathrm{E}}_{\mathrm{BaLu_2S_4}}$, kJ/mol | $T$, K | $X^{\mathrm{L}}_{\mathrm{BaLu_8S_{13}}}$ | $X^{\mathrm{S}}_{\mathrm{BaLu_8S_{13}}}$ | $\bar{G}^{\mathrm{E}}_{\mathrm{BaLu_8S_{13}}}$, kJ/mol |
| 2100 | 0.83 | 1.00 | 2.5 | 2055 | 0.83 | 1.00 | 2.6 |
| 2065 | 0.67 | 1.00 | 1.0 | 2040 | 0.67 | 1.00 | 4.6 |
| 2050 | 0.50 | 1.00 | 3.8 | 2015 (eut.) | 0.60 | 1.00 | 3.6 |
| 2020 | 0.40 | 1.00 | 3.0 | | | | |
| 2015 (eut.) | 0.40 | 1.00 | 2.2 | | | | |

**Table 7 Excess partial molar Gibbs energies of components in the $BaLu_8S_{13}$-$Lu_2S_3$ system**

| Compositions between eutectic and $BaLu_8S_{13}$ | | | | Compositions between $Lu_2S_3$ and eutectic | | | |
|---|---|---|---|---|---|---|---|
| $T$, K | $X^{\mathrm{L}}_{\mathrm{BaLu_8S_{13}}}$ | $X^{\mathrm{S}}_{\mathrm{BaLu_8S_{13}}}$ | $\bar{G}^{\mathrm{E}}_{\mathrm{BaLu_8S_{13}}}$, kJ/mol | $T$, K | $X^{\mathrm{L}}_{\mathrm{Lu_2S_3}}$ | $X^{\mathrm{S}}_{\mathrm{Lu_2S_3}}$ | $\bar{G}^{\mathrm{E}}_{\mathrm{Lu_2S_3}}$, kJ/mol |
| 2050 | 0.90 | 1.00 | 0.7 | 1995 | 0.75 | 1.00 | 1.4 |
| 2015 | 0.75 | 0.95 | −1.0 | 1975 | 0.60 | 1.00 | −1.8 |
| 1995 | 0.65 | 0.90 | −1.8 | 1950 (eut.) | 0.50 | 1.00 | −7.5 |
| 1950 (eut.) | 0.50 | 0.85 | −3.6 | | | | |

---

*The integral Gibbs energy is readily computed as $G^{\mathrm{E}} = X_{\mathrm{BaS}}\bar{G}^{\mathrm{E}}_{\mathrm{BaS}} + X_{\mathrm{BaLn_2S_4}}G$ is computed from the Hildebrand relations $\bar{G}^{\mathrm{E}} = A_{\mathrm{G}}X_{\mathrm{BaS}}X_{\mathrm{BaLn_2S_4}}$.

Between $\mathrm{BaLu_2S_4}$ and $\mathrm{Lu_2S_3}$ an intermediate compound $\mathrm{BaLu_8S_{13}}$ is interposed between the two end constituents, $\mathrm{BaLu_2S_4}$ and $\mathrm{Lu_2S_3}$. The compound melts congruently and decomposes eutectoidally. It participates in two eutectic reactions, one with $\mathrm{BaLu_2S_4}$ and the other with $\mathrm{Lu_2S_3}$. Here it is convenient to consider separately the two subsystems $\mathrm{BaLu_2S_4}$-$\mathrm{BaLu_8S_{13}}$ and $\mathrm{BaLu_8S_{13}}$-$\mathrm{Lu_2S_3}$. Data for the excess partial Gibbs energies in these two subsystems are shown in Tables 6 and 7. In Table 6, the excess integral Gibbs energy associated with the eutectic reaction is $G^{\mathrm{E}} = -3.0$ kJ/mol and the Hildebrand exchange energy* is $A_{\mathrm{G}} = -12.6$ kJ/mol. In Table 7 the same values for the second eutectic are, respectively, $G^{\mathrm{E}} = -5.6$ kJ/mol and $A_{\mathrm{G}} = -22.6$ kJ/mol. The temperature dependences of $\bar{\mathrm{G}}^{\mathrm{E}}_{\mathrm{BaLu_8S_{13}}}$ and $\bar{\mathrm{G}}^{\mathrm{E}}_{\mathrm{Lu_2S_3}}$ are again well described by linear relationships with correlations of 0.99 in both cases with $\bar{\mathrm{H}}^{\mathrm{E}}_{\mathrm{BaLur_2}}\mathrm{S_4} = -87$ kJ/mol and $\bar{\mathrm{S}}^{\mathrm{E}}_{\mathrm{BaLu_2S_4}} = -43$ J/mol K for $\mathrm{BaLu_8S_{13}}$ and $\bar{\mathrm{H}}^{\mathrm{E}}_{\mathrm{Lur_2S_3}} = -400$ kJ/mol and $\bar{\mathrm{S}}^{\mathrm{E}}_{\mathrm{Lu_2S_3}} = -200$ J/mol K for $\mathrm{Lu_2S_3}$.

## 4. Conclusion

Data from thermal analyses from $\mathrm{BaS}$-$\mathrm{Ln_2S_3}$ specimens of different compositions have been used to calculate useful thermodynamic quantities for the systems $\mathrm{BaS}$-$\mathrm{Ln_2S_3}$ with Ln = Pr, Sm, Gd, Tb, Er, and Lu. Results from these calculations show deviations of melt solutions from ideality and can be interpreted in terms of phase formation and to predict phase formation in other systems. Utility of the approach for use with other materials is implicit.

### References

1. O.V. Andreev, N.N. Parshukov, A.V. Kertman, and G.M. Kuzmicheva, Phase Diagrams of Systems $\mathrm{BaS}$-$\mathrm{Er_2S_3}$ and $\mathrm{BaS}$-$\mathrm{Lu_2S_3}$. *J. Inorg. Chem.,* Vol 43 (No. 4), 1998, p 679-683 (in Russian)
2. O.V. Andreev, N.N. Parshukov, and V.G. Bamburov, The Phase Diagrams of Systems $\mathrm{BaS}$-$\mathrm{Ln_2S_3}$ (Ln = Sm, Gd), *J. Inorg. Chem.,* Vol 43 (No. 5), 1998, p 853-857 (in Russian)
3. A.I. Efimov, Properties of Inorganic Compounds, Chemistry, Leningrad, Vol 25, 1983, p 392 (in Russian)
4. N.A. Khritohin, O.V. Andreev, A.S. Korotkov, and O.Y. Mitroshin, Thermodynamic Estimation of Melting Heats of Sufides Alkali-Earth and Rare-Earth, Proc. Conference, FAGRAN-2002 (Voronezh), 2002, p 369
5. R.G. Pearson, *J. Chem. Education,* Vol 64 (No. 7), 1987, p 561-567